Research Square

Preprints are preliminary reports that have not undergone peer review.
They should not be considered conclusive, used to inform clinical practice,
or referenced by the media as validated information.

Molecular characterization of a deep intronic TBX5 variant in a familial case of Holt-Oram syndrome

Daria Akimova

mkda6ka@mail.ru

Research Centre for Medical Genetics https://orcid.org/0009-0002-7001-4099

Tatiana Markova

Research Centre for Medical Genetics

Igor Andreev

Research Centre for Medical Genetics

Peter Sparber

Research Centre for Medical Genetics

Mikhail Skoblov

Research Centre for Medical Genetics

Vladimir Kenis

H. Turner National Medical Research Center for Children's Orthopedics and Trauma Surgery

Oxana Ryzhkova

Research Centre for Medical Genetics

Article

Keywords:

Posted Date: August 20th, 2026

DOI: https://doi.org/10.21203/rs.3.rs-10525809/v1

License: This work is licensed under a Creative Commons Attribution 4.0 International License.
Read Full License

Additional Declarations: There is no conflict of interest

Abstract

Background

Holt-Oram syndrome (HOS) is a rare autosomal dominant disorder characterized by congenital heart defects and upper-limb malformations, most commonly caused by pathogenic variants in *TBX5*. To date, only approximately 200 variants in *TBX5* have been described in association with HOS and congenital heart disease. Among the reported variants, splicing and regulatory variants are the least represented groups. In this work, we describe a familial form of HOS in a family where the father and son are carriers of a previously undescribed deep-intronic variant NM_000192.4:c.756 − 634_756-632delinsGTG in the *TBX5* gene.

Methods

The variant was identified by trio whole-genome sequencing as a variant of uncertain clinical significance. In silico analysis predicted activation of cryptic donor and acceptor splice sites, resulting in inclusion of a pseudoexon. To validate this effect, we performed RT-PCR on RNA from the father cultured skin fibroblasts, followed by targeted long-read sequencing.

Results

RNA analysis confirmed the inclusion of the pseudoexon in the father samples along with residual inclusion in control samples. PE inclusion was predicted to cause a frameshift and premature termination codon, p.(Lys253ProfsTer17). Allelic imbalance analysis demonstrated reduced expression of one *TBX5* allele, and cycloheximide-mediated inhibition of nonsense-mediated decay confirmed partial degradation of the aberrant transcript.

Conclusions

These findings confirmed the pathogenicity of the first reported deep-intronic *TBX5* variant causing HOS, which acts through a regulatory splicing mechanism, and highlight the importance of functional RNA analysis for interpreting non-coding variants.

Introduction

Holt-Oram syndrome (HOS) is a rare autosomal dominant disorder characterized by congenital cardiac malformations associated with skeletal abnormalities of the upper limbs and shoulder girdle (1). The syndrome was first described in a family in which affected members across four generations presented with limb malformations ranging from subtle defects, such as absent or triphalangeal finger-like thumbs, to upper-limb phocomelia, in combination with atrial septal defects (2). HOS is considered to show

complete penetrance with variable expressivity (2, 3). Cardiac manifestations occur in approximately 75% of patients and most commonly include septal defects (4). However, the phenotypic spectrum of HOS is not limited to the heart and upper limbs; additional anomalies, including scoliosis, growth retardation, pectus excavatum, other spinal deformities, and pulmonary malformations, have also been reported (5, 6).

In 1997, Craig T. Basson and colleagues established that HOS is caused by pathogenic variants in the *TBX5* gene (7). *TBX5* belongs to an evolutionarily conserved family of T-box genes, which are characterized by a shared DNA-binding domain known as the T-domain. These genes encode transcription factors that play key roles in the regulation of embryonic development (8, 9). Consistent with this function, *TBX5* is primarily recognized for its critical role in cardiac and forelimb morphogenesis (10).

The global prevalence of HOS is estimated to be approximately 1 in 100,000 live births worldwide, with no sex preference, supporting its classification as an orphan disease. Consistent with its rarity, the number of identified causative variants remains limited. To date, only approximately 200 variants in *TBX5* have been described in association with HOS and congenital heart disease. Among the reported variants, splicing and regulatory variants are the least represented groups. Most of these variants lack functional validation, although such validation is essential for understanding the molecular pathogenesis of HOS and for developing tailored therapeutic approaches.

Here, we report a proband with a clinical diagnosis of HOS in whom whole-genome sequencing (WGS) identified a deep-intronic variant in *TBX5*, NM_000192.4:c.756 – 634_756-632delinsGTG, inherited from his similarly affected father. Using RNA analysis combined with long-read sequencing, we demonstrated that this variant induces pseudoexon (PE) inclusion, resulting in a frameshift and predicted protein truncation. Furthermore, nonsense-mediated decay (NMD) inhibition confirmed partial degradation of the aberrant transcript. Our findings establish the pathogenicity of this deep-intronic variant and highlight the importance of functional analysis for the interpretation of non-coding variants.

Materials and Methods

Patients

The proband, a 3-year-old boy, and his parents underwent a detailed clinical examination, DNA analysis and genetic counseling at the Research Center for Medical Genetics (RCMG), Russia. All research participants gave informed consent for the clinical examination and publication of their anonymized data. The study was performed in accordance with the Declaration of Helsinki.

Whole genome sequencing

WGS was performed by the National Genetic Initiative “100,000 + Me” (NGI). Library construction was carried out using a PCR-free protocol on MGI sequencing platforms, following the standard guidelines. Paired-end sequencing (2×150 bp) was subsequently performed on a DNBSEQ-T7 genetic analyzer (MGI), yielding an average genome coverage of 36x. The resulting reads were aligned to the human reference genome (hg38) using BWA version 0.7.17-r1188. Variant calling was conducted with DeepVariant. Copy number variations (CNVs) were assessed using Manta (v.1.6.0). Variant annotation was carried out using the certified software NGS-DATA-OMICS [Beskorovayny N.S., Beskorovaynaya T.S., Ryzhkova O.P., Shchoka E.V., Vizerov T.V., Stepanova A.A., Shchagina O.A., Polyakov A.V., Kutsev S.I. Computer Program Registration Certificate No. RU 2025685783. Russian Federation, registered September 26, 2025 (filed August 14, 2025)].

Read quality was evaluated with FastQC (v.0.11.9). Identified genetic variants were named according to HGVS nomenclature (v.21.1.2). Population allele frequencies were obtained from the 1000 Genomes Project and gnomAD (v3.1.2, v.4.0.0). Clinical significance of the variants was assessed using ACMG guidelines (11) (12).

Segregation analysis

Genomic DNA extracted from peripheral blood samples of the proband and his parents using the QIAamp DNA Blood Mini Kit (QIAGEN, Venlo, Netherlands) according to the manufacturer’s instructions was used as a template. PCR amplification was performed using the ProFlex PCR System (Applied Biosystems), and the resulting PCR products were visualized by agarose gel electrophoresis. The PCR products were subsequently subjected to in-house Sanger sequencing (Genterra). The following primers were used for validation and segregation analysis of the NM_000192.4:c.756 – 634_756-632delinsGTG variant: forward, 5'-GATGGGGCCTGAATTGGGAG-3'; reverse, 5'-TAAGGTGGGGCTCAGGTCAT-3'.

RNA analysis

Total RNA was extracted from skin fibroblasts derived from the proband’s father. All cell cultures were obtained from and deposited in the Moscow Branch of the Biobank “All-Russian Collection of Biological Samples of Hereditary Diseases”.

RNA extraction was performed on an AutoPure S32 automated station using the MagPure Universal RNA Kit, according to the manufacturer’s instructions. Reverse transcription was performed with oligo-dT primers using the Reverse Transcription System (Dialat, Russia), in accordance with the manufacturer’s protocol. The quality of the obtained cDNA was assessed by qPCR analysis of housekeeping genes.

To investigate the effect of the NM_000192.4:c.756 – 634_756-632delinsGTG variant on mRNA structure, the target *TBX5* locus was amplified using the following primers: forward, 5'-TGGACATTGTACCTGCCGAC-3'; reverse, 5'-CCAGCTCCTATGCTGGGTTT-3'. The resulting RT-PCR products were subsequently subjected to targeted long-read sequencing.

Nonsense-mediated decay inhibition in fibroblast cultures

Fibroblasts from the proband's father and healthy donors (controls) were seeded at a density of 3×10^5 cells per well in 6-well plates 24 h before treatment. Cells were cultured in high-glucose DMEM supplemented with 10% fetal bovine serum at 37°C in a 5% CO_2 atmosphere. At the time of treatment, cell confluence was approximately 80%.

Two culture conditions were used: control medium to assess the potential effect of the solvent (untreated, UT) and medium supplemented with cycloheximide (CHX). CHX was added at a final concentration of 50 µg/mL, corresponding to a 1:1000 dilution of the stock solution. Fibroblasts from the proband's father and control fibroblasts were incubated in parallel either in the presence of CHX or in control medium without CHX, containing DMSO at a 1:1000 dilution, for 24 h at 37°C in a 5% CO_2 atmosphere.

After incubation, the cells were visually examined under a microscope to confirm the absence of apparent toxic effects. The culture medium was then removed, and the cells were lysed directly in the wells of the 6-well plate using RLT buffer (Magen) supplemented with β-mercaptoethanol. Samples were immediately frozen and stored at -80°C until subsequent total RNA extraction.

The efficiency of NMD inhibition was assessed using a control locus in the *SRSF3* gene, which contains alternative exon 4 in the NMD-sensitive isoform NR_036610.1. RT-PCR products were visualized and isoform ratios were evaluated by electrophoresis in a 2% agarose gel. The following primers were used for amplification of the control locus: forward, 5'-CACTATGTGGCTGCCGTGTA-3'; reverse, 5'-ATCGGGACGGCTTGTGATTT-3'.

Long-read sequencing of targeted RT-PCR products

Long-read sequencing of PCR amplicons was performed using Oxford Nanopore Technology (ONT). Coverage of the target locus exceeded 300× in both the proband's father and control samples. Reads were aligned to the human reference genome hg38 hisat2 v.2.2.1. FASTQ quality assessment was performed using FastQC v0.12.1 and NanoPlot v1.46.1. Splice junctions were visualized as Sashimi plots in the Integrative Genomics Viewer (IGV).

Results

Clinical findings

The proband was referred to a geneticist at the age of 2 years and 5 months because of congenital malformations of both upper limbs, presumably inherited from his similarly affected father. He was born from the third pregnancy of a non-consanguineous couple. HOS (OMIM #142900) had previously been suspected in the father on the basis of combined cardiac and upper-limb malformations. At the age of 6 years, the father underwent surgical repair of a primary atrial septal defect. His phenotype included

ectrodactyly and a rudimentary thumb of the right hand, which had been surgically corrected, aplasia of the left thumb, left-sided radial club hand, flexion contracture of the left elbow joint, hypoplasia of the forearm bones, and pectus excavatum (Fig. 1A). During pregnancy planning, he underwent a series of genetic tests, including Sanger sequencing of *TBX5*, clinical exome sequencing and chromosomal microarray analysis; however, none identified a causative variant.

The family obstetric history was complicated by previous terminations of pregnancy for medical indications. The first pregnancy was terminated at 14–15 weeks of gestation after the detection of fetal limb anomalies, including aplasia of the right radius, aplasia of the left forearm bones, syndactyly, and bilateral thumb aplasia. Karyotyping of post-abortion fetal material showed a normal male karyotype, 46,XY. The second pregnancy was terminated at 17–18 weeks of gestation following the detection of fetal hydrops, a congenital heart defect, micrognathia, and mosaic trisomy 18.

The child was born with a birth weight of 3470 g, a length of 54 cm, and Apgar scores of 5/7/8. At birth, hypoplasia of the left upper limb and both hands was noted. On the second day of life, the infant was transferred to the intensive care unit because of tachypnea and received continuous positive airway pressure oxygen therapy. Echocardiography performed at that time revealed multiple congenital heart defects, including hypoplasia of the aortic arch, coarctation of the aorta, a large atrial septal defect of the common atrium type, a muscular ventricular septal defect, patent ductus arteriosus, increased pulmonary blood flow, and pulmonary hypertension.

At the age of 3 months, the child underwent surgical closure of the atrial septal defect and reconstruction of the aortic arch. Delayed motor milestones were observed: head control was achieved at 4 months, unsupported sitting at 10 months, and independent walking at 18 months. Psychomotor and speech development were age-appropriate.

At the age of 6 months, anteroposterior radiographs of the chest, shoulder girdles, and upper arms revealed an increased cardiothoracic ratio exceeding 50%, with the cardiac width measuring more than half of the thoracic width, together with right atrial dilatation and enlargement of the pulmonary artery. Additional findings included hypoplastic glenoid cavities with relatively long acromial processes, horizontally oriented ribs, and normal morphology of the left elbow joints. Pulmonary vascularity was increased. Palmar-view radiographs of the hands and wrists showed mild radial deviation of both hands, absent ossification of the carpal bones, and hypoplasia of the first metacarpals and thumb phalanges (Fig. 1B).

On examination at the age of 2 years and 5 months, the proband's growth parameters were appropriate for age: height, 88 cm (-0.76 SDS); body weight, 12 kg (-1.02 SDS). He had hypoplasia of the left forearm, bilateral thumb hypoplasia, and deformity of the index fingers, more pronounced on the left. Both thumbs and index fingers showed a limited range of motion and axial deviation (Fig. 1C).

Based on the medical history, clinical examination, and diagnostic findings, HOS was suspected in both the proband and his father. To confirm the diagnosis, trio WGS was performed.

DNA analysis

Trio WGS followed by analysis of a bioinformatic gene panel covering the complete sequences of 756 genes associated with congenital arthrogryposis and other congenital malformation was performed in the reported family. In total, 4,147 variants met the predefined quality criteria: PASS filter status, DP > 4, and maximum population frequency in gnomAD v4.0.0 < 0.06. Among these, only one variant was consistent with both the expected inheritance pattern and the clinical phenotype: a previously undescribed intronic variant in *TBX5* (c.756 − 634_756-632delinsGTG), located in intron 7. The variant was inherited from the father, who presented with a similar phenotype, and was absent from the gnomAD v4.1.0 population database.

In-silico splicing prediction tools provided discordant results: SpliceAI (13) predicted the variant to be likely splice-affecting, whereas SPiP (13, 14) and Squirls (15) classified it as neutral. Given that pathogenic variants in *TBX5* are the primary molecular cause of HOS (10), this variant was reported as a variant of uncertain significance (VUS) according to the ACMG 2015 criteria, with the following evidence applied: PM2, PP1, and PP4.

RNA analysis

To investigate the pathogenicity of the c.756 − 634_756-632delinsGTG variant, we first performed bioinformatic analysis using SpliceAI. The variant was predicted to activate cryptic splice sites within intron 7, including both donor (Δ score = 0.37) and acceptor (Δ score = 0.40) sites, potentially resulting in the inclusion of a 53-nucleotide PE (Fig. 2A).

Additional in silico analysis of the c.756 − 634_756-632delinsGTG variant using AlphaGenome (16), with the RNA_SEQ and SPLICE_SITE_USAGE output metrics, also supported possible PE inclusion. In the alternative allele track, an additional exonic region within intron 7 was incorporated into the predicted mRNA, as shown by the RNA-seq coverage track, together with activation of both cryptic donor and acceptor splice sites. These changes were not observed in the reference allele (Fig. 2A).

To validate the in silico predictions and assess the effect of the c.756 − 634_756-632delinsGTG variant on *TBX5* mRNA structure and expression, we developed an RT-PCR assay enabling amplification of exons 6 through 9 of the *TBX5* transcript. According to the GTEx database, *TBX5* expression in fibroblasts is sufficient for RNA analysis (2.071 TPM). Therefore, the analysis was performed using mRNA isolated from cultured skin fibroblasts of the proband's father and a healthy donor, followed by cDNA synthesis, amplification of the target locus, and long-read sequencing of the resulting PCR products.

Analysis of the long-read sequencing data revealed two transcript types in both the proband's father and the healthy control: the reference transcript corresponding to isoform NM_000192.4 and a transcript with PE inclusion in intron 7, consistent with the bioinformatic predictions (Fig. 2B). Sashimi plot

analysis showed that the PE inclusion rate in control samples did not exceed 0.2%, whereas in the proband's father, PE-containing transcripts accounted for 22% of all *TBX5* transcripts (Fig. 2C).

Inclusion of this PE is predicted to cause a frameshift and generate a premature termination codon. If translated, the aberrant transcript would produce a truncated *TBX5* protein shortened by 250 amino acids, p.(Lys253ProfsTer17).

The amplified *TBX5* mRNA locus from the proband's father contained two common heterozygous variants, rs6489956 and rs883079, which enabled quantification of possible allelic imbalance. Analysis of these variants at the RNA level revealed allelic ratios of 73%/27% and 27%/73% (ref/alt), respectively, confirming reduced expression of one *TBX5* allele (Fig. 2D).

Variants that introduce premature termination codons can trigger degradation of aberrant transcripts through NMD (17, 18). Since RNA analysis demonstrated that the c.756 − 634_756-632delinsGTG variant leads to premature translation termination, we hypothesized that PE-containing transcripts are degraded by NMD. To evaluate the contribution of NMD to the reduced expression of the aberrant allele, we inhibited NMD using CHX in cultured fibroblasts from the proband's father and a healthy control, followed by analysis of the cDNA target locus as described above.

After NMD inhibition, the relative level of the aberrant PE-containing transcript in the proband's father increased from 22% to 37% of the total *TBX5* transcript pool, confirming that the aberrant transcript undergoes NMD. The remaining fraction of aberrant mRNA appears to escape NMD and may be translated into the truncated p.(Lys253ProfsTer17) protein. Notably, the level of PE-containing transcripts also increased in control samples, from 0.3% in untreated cells to 3% in CHX-treated cells, indicating low-level residual PE inclusion under normal conditions.

Using data on the two common heterozygous variants, rs6489956 and rs883079, we also performed long-read phasing to assess the efficiency of pseudoexonization. Phasing analysis of ONT data from untreated cultured fibroblasts (without CHX treatment) revealed that approximately 10% of reads originating from transcripts expressed from the allele carrying the c.756-634_756-632delinsGTG variant lacked the pseudoexon and represented full-length transcripts. Indeed, since this variant is regulatory in nature, it is not expected to lead to pseudoexon inclusion in 100% of cases.

Thus, based on the RNA analysis results, the c.756 − 634_756-632delinsGTG variant was classified as likely pathogenic according to the ACMG/AMP recommendations and was considered causative in this family (PM2, PVS1_Strength (RNA), PP1) (11, 12).

Discussion

In this study, we report a previously undescribed deep-intronic variant in *TBX5*, c.756 − 634_756-632delinsGTG, identified by trio WGS in a family with clinical features of HOS. The variant was inherited from the proband's father, who presented with a similar but milder phenotype. Using a combination of

bioinformatic prediction, targeted RT-PCR, ONT sequencing, and NMD inhibition experiments, we provide evidence that this variant leads to PE inclusion. Inclusion of this PE results in a frameshift and the formation of a premature termination codon, p.(Lys253ProfsTer17), followed by NMD of a fraction of the aberrant transcript.

The family described in this study provides a striking illustration of the well-known phenomenon of variable expressivity in HOS (19). Although HOS is characterized by complete penetrance (20, 21), its clinical manifestations may vary widely, even within the same family (22).

In our study, the proband and his father also show different severity of clinical manifestations. Skeletal anomalies are significantly more pronounced in the proband's father: he had ectrodactyly, a rudimentary thumb of the right hand that had undergone surgical reconstruction, aplasia of the left thumb, left-sided radial club hand, flexion contracture of the left elbow joint, hypoplasia of the forearm bones, and pectus excavatum. At the same time, the proband's upper-limb malformations are quite mild, which is one of the reasons why the phenotype was missed during prenatal ultrasound. On the other hand, the severity of cardiac pathology in the proband is substantially higher than in his father: the proband was diagnosed on the second day of life with severe combined congenital cardiac abnormalities requiring surgical intervention.

Moreover, the family history included a previous pregnancy that was terminated because of severe fetal limb malformations. This may represent the most severe end of the phenotypic spectrum in this family, possibly influenced by additional genetic factors.

In the family described here, the pathogenic variant in *TBX5* is predicted to alter and truncate the C-terminal region of the protein, p.(Lys253ProfsTer17). This region contains the transactivation domain and mediates protein–protein interactions with LMP4 and TAZ. Experiments using a yeast one-hybrid system and, subsequently, mammalian ECL-2 cells showed that even a three-amino-acid deletion at positions 349–351 within the transactivation domain completely abolishes protein function, whereas deletion of residues 325–327 results in cytoplasmic mislocalization of TBX5, consistent with this sequence acting as a nuclear localization signal (23).

Although numerous nonsense and frameshift variants in *TBX5* have been described (24), deep-intronic variants causing PE inclusion and thereby leading to a frameshift and protein truncation have not yet been reported yet in HOS.

Notably, the c.756 – 634_756-632delinsGTG variant itself does not directly create or strengthen canonical splice donor or acceptor sites, as judged by SpliceAI and AlphaGenome predictions. This observation suggests that the variant is more likely to exert a regulatory effect, either by disrupting an exonic splicing silencer (ESS) or by creating a splicing enhancer (ESE). However, our in silico analyses did not allow us to distinguish between these two possibilities, as no candidate silencer motif was clearly identified in the vicinity of the variant using available prediction tools (Sup. Figure 1). Interestingly, both SpliceAI and AlphaGenome also predicted that several other variants within the same genomic

locus could potentially lead to pseudoexon inclusion, implying that this region may be particularly sensitive to sequence changes affecting splicing regulation.

Supplementary Fig. 1.

Interestingly, cDNA sequencing analysis revealed a small fraction of PE-containing transcripts, not only in the proband's father but also in control samples from a healthy donor. Moreover, after CHX treatment, the proportion of these transcripts increased, as expected, in the proband's father, but also increased in the control sample, from 0.2% to 5%.

Based on these data, it may be speculated that unproductive splicing contributes to the regulation of *TBX5* gene expression (23, 25). By analogy with genes encoding SR proteins, such a mechanism may help maintain an appropriate expression level of the regulated gene. Indeed, Romain Georges and colleagues showed that *TBX5* undergoes complex post-transcriptional regulation, generating several splice isoforms, including a shortened isoform with an altered C-terminus. This shortened isoform retains DNA-binding capacity, but its interaction with other proteins, such as GATA4, is altered, which may have important functional implications (25, 26).

Thus, the basal level of PE inclusion detected in control samples may not represent a splicing error, but rather a physiological regulatory mechanism. This mechanism may involve the production of a minor fraction of NMD-targeted transcripts, allowing cells to dynamically fine-tune *TBX5* protein homeostasis.

It is worth mentioning that the proband's father had previously undergone WGS during pregnancy planning, but no causative variant in *TBX5* was identified at that time. This case illustrates the challenges associated with the detection and interpretation of deep-intronic variants, which in this family became apparent only after trio sequencing. However, according to current recommendations, such variants are often classified as VUS, which is insufficient to confirm a molecular diagnosis or guide reproductive decision-making. In many cases, functional testing remains the only approach that can provide sufficient evidence to reclassify such variants as causative.

Here, using mRNA analysis, we showed that the c.756 – 634_756-632delinsGTG variant in *TBX5* leads to PE inclusion and, consequently, degradation of a fraction of aberrant transcripts through the NMD pathway. The remaining fraction appears to escape NMD and may be translated into a truncated, non-functional protein. Our results confirm the pathogenicity of the first reported deep-intronic variant in *TBX5* and underscore the importance of functional analysis for the interpretation of non-coding variants.

Abbreviations

HOS
Holt-Oram syndrome
WGS
whole-genome sequencing

PE
pseudoexon
NMD
nonsense-mediated decay
RCMG
Research Center for Medical Genetics
NGI
National Genetic Initiative (“100,000 + Me”)
BWA
Burrows-Wheeler Aligner
CNV
copy number variation
CHX
cycloheximide
UT
untreated
ONT
Oxford Nanopore Technology
IGV
Integrative Genomics Viewer
VUS
variant of uncertain significance
ESS
exonic splicing silencer
ESE
exonic splicing enhancer

Declarations

Ethics approval and consent to participate

All research participants gave informed consent for the clinical examination and publication of their anonymized data. The study was performed in accordance with the Declaration of Helsinki and was approved by the Institutional Review Board of the Research Centre for Medical Genetics (approval no. 11/23.11.2021).

Competing interests

The authors declare that they have no competing interests.

Consent for publication

All research participants gave written informed consent to the clinical examination and the publication of their anonymized data. Since the proband is under 18 years old, informed consent for clinical examination and publication was obtained from their parents.

Funding

This work was supported by the Russian Science Foundation (project № 25-65-00031)

Author contributions

DA – conception, data curation, formal analysis, investigation, writing - original draft, TM - data curation, investigation, writing - review and editing, IA - investigation, OR - writing - original draft, VK – writing - review and editing, PS – supervision, MS – conception, data curation, formal analysis, writing - review and editing, supervision. All authors reviewed the final manuscript.

Acknowledgements

We thank the patient and his family for their participation in this study.

The research was performed using the facilities and equipment of the "Genome" Shared Resource Centre at the Research Centre for Medical Genetics (Moscow, Russia).

Availability of data and materials

The *TBX5* variant NM_181486.4:c.756 − 634_756-632delinsGTG has been deposited in ClinVar with accession number VCV004819998.1.

References

1. Hurst JA, Hall CM, Baraitser M. The Holt-Oram syndrome. J Med Genet. 1991;28(6):406–10.
2. Holt M, Oram S. Familial heart disease with skeletal malformations. Br Heart J. 1960;22(2):236–42.
3. Allurwar H, Agrawal A, Ingole A, Sapkale B. Clinical features, molecular pathogenesis, diagnosis and management of Holt-oram Syndrome: A narrative review. J Clin Diagn Res [Internet]. 2026; Available from: https://www.jcdr.net/article_fulltext.asp?issn=0973-709x&year=2026&volume=20&issue=1&page=GE01&issn=0973-709x&id=22205

4. Kumar R, Mahapatra SS, Datta M, Hoque A, Datta S, Ghosh S, et al. Holt-oram syndrome in adult presenting with heart failure: a rare presentation. Case Rep Cardiol. 2014;2014:130617.
5. Vanlerberghe C, Jourdain AS, Ghoumid J, Frenois F, Mezel A, Vaksmann G, et al. Holt-Oram syndrome: clinical and molecular description of 78 patients with TBX5 variants. Eur J Hum Genet. 2019;27(3):360–8.
6. Atlas I, Zagdan S, Megzari M, Arous S, Drighil A. When the heart and hands tell a story: an intriguing case of Holt-Oram syndrome. Egypt Heart J. 2024;76(1):117.
7. Basson CT, Bachinsky DR, Lin RC, Levi T, Elkins JA, Soults J, et al. Mutations in human TBX5 [corrected] cause limb and cardiac malformation in Holt-Oram syndrome. Nat Genet. 1997;15(1):30–5.
8. Kispert A, Koschorz B, Herrmann BG. The T protein encoded by Brachyury is a tissue-specific transcription factor. EMBO J. 1995;14(19):4763–72.
9. Basson CT, Huang T, Lin RC, Bachinsky DR, Weremowicz S, Vaglio A, et al. Different TBX5 interactions in heart and limb defined by Holt-Oram syndrome mutations. Proc Natl Acad Sci U S A. 1999;96(6):2919–24.
10. Steimle JD, Moskowitz IP. TBX5: A Key Regulator of Heart Development. Curr Top Dev Biol. 2017;122:195–221.
11. Richards S, Aziz N, Bale S, Bick D, Das S, Gastier-Foster J, et al. Standards and guidelines for the interpretation of sequence variants: a joint consensus recommendation of the American College of Medical Genetics and Genomics and the Association for Molecular Pathology. Genet Med. 2015;17(5):405–24.
12. Walker LC, Hoya M de la, Wiggins GAR, Lindy A, Vincent LM, Parsons MT, et al. Using the ACMG/AMP framework to capture evidence related to predicted and observed impact on splicing: Recommendations from the ClinGen SVI Splicing Subgroup. Am J Hum Genet. 2023;110(7):1046–67.
13. Jaganathan K, Kyriazopoulou Panagiotopoulou S, McRae JF, Darbandi SF, Knowles D, Li YI, et al. Predicting Splicing from Primary Sequence with Deep Learning. Cell. 2019;176(3):535–48.e24.
14. Leman R, Parfait B, Vidaud D, Girodon E, Pacot L, Le Gac G, et al. SPiP: Splicing Prediction Pipeline, a machine learning tool for massive detection of exonic and intronic variant effects on mRNA splicing. Hum Mutat. 2022;43(12):2308–23.
15. Danis D, Jacobsen JOB, Carmody LC, Gargano MA, McMurry JA, Hegde A, et al. Interpretable prioritization of splice variants in diagnostic next-generation sequencing. Am J Hum Genet. 2021;108(11):2205.
16. Avsec Ž, Latysheva N, Cheng J, Novati G, Taylor KR, Ward T, et al. Advancing regulatory variant effect prediction with AlphaGenome. Nature. 2026;649(8099):1206–18.
17. Karousis ED, Nasif S, Mühlemann O. Nonsense-mediated mRNA decay: novel mechanistic insights and biological impact. Wiley Interdiscip Rev RNA. 2016;7(5):661–82.

18. Miller JN, Pearce DA. Nonsense-mediated decay in genetic disease: friend or foe? Mutat Res Rev Mutat Res. 2014;762:52–64.
19. Brassington AME, Sung SS, Toydemir RM, Le T, Roeder AD, Rutherford AE, et al. Expressivity of Holt-Oram syndrome is not predicted by TBX5 genotype. Am J Hum Genet. 2003;73(1):74–85.
20. Newbury-Ecob RA, Leanage R, Raeburn JA, Young ID. Holt-Oram syndrome: a clinical genetic study. J Med Genet. 1996;33(4):300–7.
21. Ross SB, Bagnall RD, Yeates L, Sy RW, Semsarian C. Holt-Oram syndrome in two families diagnosed with left ventricular noncompaction and conduction disease. HeartRhythm Case Rep. 2018;4(4):146–51.
22. Walencka Z, Jamsheer A, Surmiak P, Baumert M, Jezela-Stanek A, Witek A, et al. Clinical expression of Holt-Oram syndrome on the basis of own clinical experience considering prenatal diagnosis. Ginekol Pol. 2016;87(10):706–10.
23. Zaragoza MV, Lewis LE, Sun G, Wang E, Li L, Said-Salman I, et al. Identification of the TBX5 transactivating domain and the nuclear localization signal. Gene. 2004;330:9–18.
24. Møller Nielsen AK, Dehn AM, Hjortdal V, Larsen LA. TBX5 variants and cardiac phenotype: A systematic review of the literature and a novel variant. Eur J Med Genet. 2024;68:104920.
25. Fair B, Buen Abad Najar CF, Zhao J, Lozano S, Reilly A, Mossian G, et al. Global impact of unproductive splicing on human gene expression. Nat Genet. 2024;56(9):1851–61.
26. Georges R, Nemer G, Morin M, Lefebvre C, Nemer M. Distinct expression and function of alternatively spliced Tbx5 isoforms in cell growth and differentiation. Mol Cell Biol. 2008;28(12):4052–67.

Figures

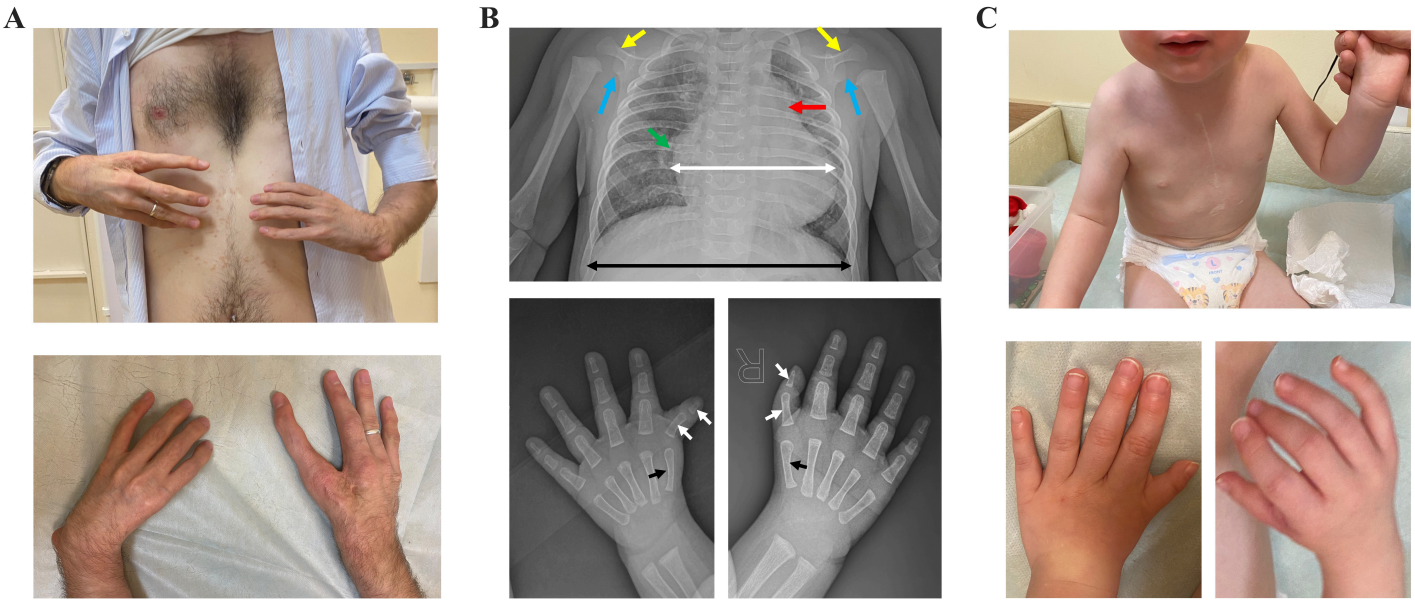


Figure 1

Clinical presentation of the affected father and child with Holt-Oram syndrome.

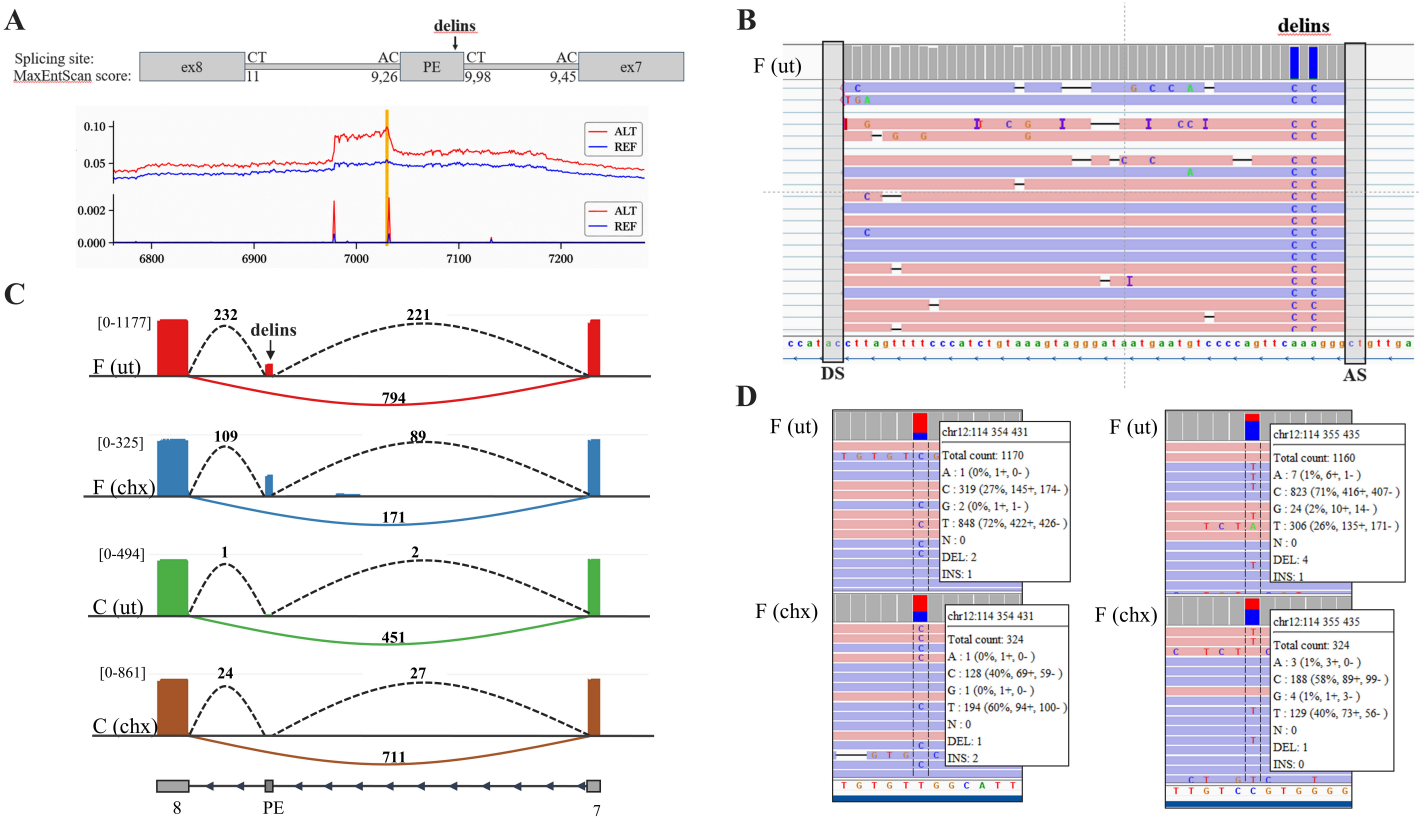


Figure 2

Bioinformatic prediction and functional analysis results of the c.756-634_756-632delinsGTG variant in the TBX gene.

Supplementary Files

This is a list of supplementary files associated with this preprint. Click to download.

- Supplementaryfigure1.jpg